Catalysis by Mixed Oxide Perovskites. I. Hydrogenolysis of Ethylene and Ethane on $LaCoO_3$

Kenji Ichimura,* Yasunobu Inoue, and Iwao Yasumori
Department of Chemistry, Tokyo Institute of Technology, Ookayama, Meguro-ku, Tokyo 152
(Received November 8, 1979)

Catalysis by a mixed oxide with a perovskite structure, $LaCoO_3$, was studied for the hydrogenolysis of ethylene and ethane at temperatures 300—600 K using the hydrogen-excess mixtures. The high and stable activity was obtained by evacuating $LaCoO_3$ at 600 K. Ethylene hydrogenolysis above 420 K proceeded consecutively *via* the intermediate, ethane, to produce methane, whereas only the hydrogenation to form ethane occurred below 420 K. Different temperature dependence of the rate was observed, *i.e.*, the activation energy of -19.3 kJ·mol^{-1} in the range 420—600 K and 33.6 kJ·mol^{-1} in the range 300—420 K. The mechanistic analysis and tracer study using D_2 showed that the slow step of the hydrogenation shifts, with increasing temperature, from the adsorption of hydrogen to the surface reaction between hydrogen atom and ethyl radical. The hydrogenolysis of ethane produced only methane and no ethylene was observed in gas phase; the reaction orders with respect to hydrogen and ethane pressures were, respectively, -0.5 and 1.0. In the reaction with D_2, methane [D_4] was the main product and an equilibrium among the formed H_2, HD, and D_2 was quickly established. The adsorption of ethane to undergo the rupture of the carbon-carbon bond and to form monocarbon species was proposed to be a slow step. The catalytic activities of the component oxides, La_2O_3 and Co_2O_3, were also examined for a comparison. The structure and electronic states of $LaCoO_3$ were investigated by means of X-ray diffraction and X-ray photoelectron spectroscopy in connection with the catalytic activity. It was proposed that the hydrogenation proceeded mainly on a pair of La^{3+} and O^{2-} ions, whereas the hydrogenolysis was accelerated by the Co^{3+} ion; the (110) plane is suggested to be the most favorable for the catalysis.

Recently, the mixed oxides which have a perovskite structure have been recognized as promising catalysts for the reactions involving hydrogen such as the equilibration between H_2 and D_2, the hydrogenation and isomerization of olefins and the hydrogenolysis of hydrocarbons and also as suitable ones for the fundamental research of catalytic activity because of their well-defined structures.[1-7] It has been theoretically shown that the valence band structures of some perovskites are similar to those of transition metals.[8-11] Among these perovskites, those containing the lanthanoid elements R, $RCoO_3$, were reported to be more active for the hydrogenolysis of *cis*-2-butene than several kinds of transition metals.[1] We have found that $LaCoO_3$ catalyzed the hydrogenolysis of ethylene and ethane to produce methane. The hydrogenolysis of the hydrocarbons on this perovskite, however, has not been studied in detail, and thus the function of the catalyst has not been revealed yet.

In the present work, being the first one in our series, the detailed kinetic study for the hydrogenolysis of ethylene and ethane was performed, and was supplemented by the analysis of deuterium distributions in the reaction with deuterium. The crystal and electronic structures of the oxide were examined by X-ray diffraction and X-ray photoelectron spectroscopy (XPS). On the basis of the obtained results, the structures of the active site for the hydrogenation and hydrogenolysis were discussed.

Experimental

Material. $LaCoO_3$ was prepared by calcining the mixed hydroxides of La and Co at 1170 K for 3 h and then 1370 K for more than 12 h. The hydroxides were coprecipitated from the mixture of equimolar solutions of $La(NO_3)_3 \cdot 6H_2O$ and $Co(NO_3)_2 \cdot 6H_2O$ by adding an aqueous solution of ammonia and the precipitate was washed with distilled water and dried at 330 K. The X-ray diffraction pattern of the calcined product coincided with that of $LaCoO_3$ reported by Askham *et al.*[12] and any other compounds were not detected. The surface area of the catalyst was estimated at 0.33 m^2·g^{-1} by BET method using Kr adsorption at 77 K.

X-Ray photoelectron spectra of the catalyst were recorded on a Hewlett-Packard 5950A ESCA spectrometer with monochromatized Al $K\alpha$ radiation (1486.6 eV) in an ultra high vacuum of 10^{-9} Torr (1 Torr=133.3 Pa). An electron flood gun was used to compensate the charging-up shifts of the spectra due to photoelectron emission. The values of observed binding energies were corrected using that of C ls, 284.7 eV, as a standard.

The property of synthesized $LaCoO_3$ was examined simultaneously by DTA and TGA using a Rigaku-Denki thermal analyser in air for the sample of 50 mg which was inserted in a platinum vessel together with the reference alumina. When the catalyst was heated from 300 to 1300 K and then cooled to 300 K at a rate of 10 K·min^{-1}, two weak endothermic peaks appeared around 610 and 910 K, accompanied by the respective decreases of 0.03 and 0.06% in weight. Further, a strong endothermic peak appearing around 1190 K with increasing temperature caused a decrease of 0.21% in weight. The endothermic change at 1190 K was reversible and attributed to the first order transformation of the crystal resulting in the elimination of oxygen. Before and after the DTA and TGA measurements, no change of X-ray diffraction pattern was observed. From the $LaCoO_3$ sample which was prepared in air by calcining at 1370 K, H_2O, CO, and CO_2 were desorbed on heating; H_2O appeared around 540 and 600 K, while CO and CO_2 desorbed around 410 and 590 K. Samples after cooling to 300 K *in vacuo* evolved scarcely any gas on the second heating up to 800 K.

Hydrogen (99.99% pure), deuterium (99.6%), methane (99.95%), ethylene (99.8%), ethane (99.7%), and *cis*-2-butene (99%) were purchased from Takachiho Chem. Ind., Ltd. and used without further purification.

Procedure. Kinetic studies were carried out in the reaction temperatures from 300 to 600 K using a closed circulation system connected to a high vacuum line. The catalyst sample, 100 to 300 mg in weight, was evacuated in a reaction tube at various temperatures between 300

Table 1. The reaction of ethylene with deuterium

I[a]	Ethylene	Ethane	Methane	Hydrogen	II[b]	Ethylene	Ethane	Hydrogen
D_0	31.9%	3.3%	1.4%	0.2%	D_0	19.5%	11%	1%
D_1	28.5%	10.6%	29.1%	8.4%	D_1	42.8%	25%	4%
D_2	38.5%	14.3%	3.5%	91.4%	D_2	28.8%	32%	95%
D_3	0 %	19.5%	24.1%		D_3	8.1%	22%	
D_4	1.1%	24.9%	42.0%		D_4	0.8%	9%	
D_5		16.4%			D_5		2%	
D_6		11.1%			D_6		0%	

a) Reaction I. Reaction temperature=573 K, conversion=24%, $P_{C_2H_4}=10.0$ Torr, $P_{D_2}=103.5$ Torr.
b) Reaction II. Reaction temperature=353 K, conversion=42%, $P_{C_2H_4}=10.0$ Torr, $P_{D_2}=113.1$ Torr.

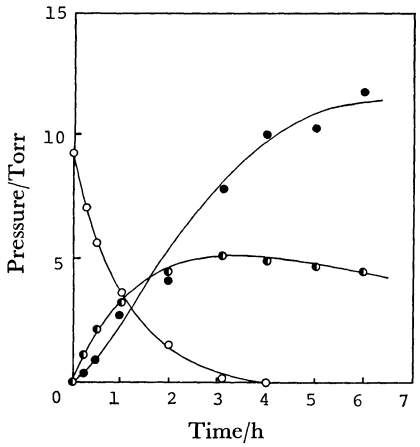

Fig. 1. Reaction of ethylene with H_2 at 573 K.
○: C_2H_4, ◐: C_2H_6, ●: CH_4.

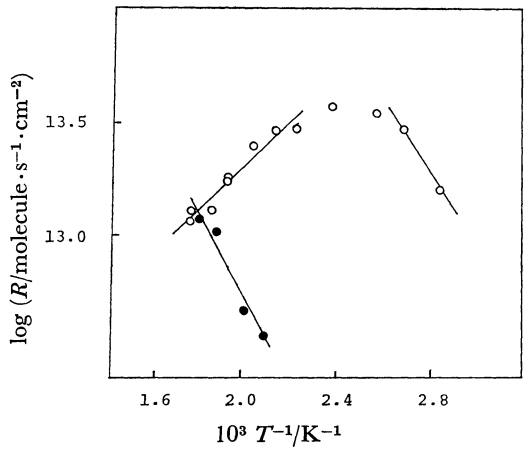

Fig. 2. Arrhenius plots for the hydrogenation of ethylene and the hydrogenolysis of ethane.
$P_{C_2H_4}=P_{C_2H_6}=10$ Torr, $P_{H_2}=100$ Torr.
○: Hydrogenation, ●: hydrogenolysis.

and 800 K for 1 to 6 h. When the catalyst was evacuated at 600 K for 1 h before each run, the activity was satisfactorily reproduced in successive ten kinetic runs and remained constant on heating the catalyst up to 800 K under vacuum.

The partial pressures of hydrocarbons were changed from 5 to 15 Torr and those of hydrogen and deuterium from 50 to 150 Torr. The composition of the reaction products was determined gas-chromatographically for the sample taken out periodically from the reaction system during the course of reaction. In addition to the hydrogenolysis of ethylene and ethane, the same reactions with D_2, the exchange reaction between methane and D_2, the equilibration of H_2 and D_2 were also examined. These reaction mixtures were analyzed by means of a mass spectrometer, Hitachi RMU-7M, and a gas chromatograph was used to analyze the isotopic molecules of hydrogen, H_2, HD, and D_2.

A preliminary study on the reaction of *cis*-2-butene (10 Torr) with hydrogen (100 Torr) over $LaCoO_3$ at 573 K confirmed that the hydrogenolysis and isomerization of butene took place simultaneously to form the main product, methane and butene isomers, as previously reported by Pedersen and Libby.[1]

Results

Hydrogenolysis of Ethylene and Ethane. Figure 1 shows the change in the gas-phase composition with time in the reaction of ethylene with hydrogen at 573 K. Ethane and methane were produced during the course of hydrogenolysis. The solid lines in the figure are the simulated curves by assuming the consecutive reaction pathway from ethylene to methane *via* an intermediate, ethane, as is described later in detail. The reaction at temperatures lower than 420 K gave only ethane as the product. Figure 2 shows the change in the initial rate of ethylene consumption with reaction temperature. The maximum in the rate appeared at about 420 K. The apparent activation energy was estimated at 33.6 kJ·mol^{-1} below 420 K and −19.3 kJ·mol^{-1} above 420 K. The kinetics of the reaction was studied at 353 and 573 K to clarify the nature of the reaction in the respective temperature ranges above and below 420 K. The rates of ethylene consumption at 573 K and 353 K are respectively expressed as

$$R_{573} = kP_{C_2H_4}P_{H_2} \quad (1)$$

and

$$R_{353} = k'P^0_{C_2H_4}P_{H_2}, \quad (2)$$

where k and k' denote the rate constants and P_i represents the partial pressure of molecule i (i=C_2H_4 or H_2).

The kinetic study of the ethane hydrogenolysis was carried out at temperatures between 473 K and 573 K. Methane was the sole product of the hydrogenolysis, and ethylene was not detected during the course of reaction. The rate of ethane consumption was given by

$$R = k^*P_{C_2H_6}P_{H_2}^{-0.5}, \quad (3)$$

with the activation energy of 34.9 kJ·mol^{-1} as shown in Fig. 2.

Isotopic Exchange Reactions of Ethylene, Ethane, or Methane with Deuterium and Equilibration between Hydrogen and Deuterium. Reaction of ethylene with D_2 was investigated at 353 K and 573 K. The observed deuterium distributions are summarized in Table 1. In the reaction at 573 K, no significant kinetic isotope effect was observed. The deuterium atoms were quite widely distributed in ethylene, ethane, and methane, whereas the produced HD and H_2 were in equilibrium with D_2 during the course of reaction. On the other hand, in the reaction at 353 K, the normal isotope effect was observed; the rate of ethylene hydrogenation with H_2 was about twice as large as that with D_2. The composition among H_2, HD, and D_2 in the gas phase was far from an equilibrium value.

The reaction of ethane with D_2 at 573 K produced methane[D_4] as main product but a negligibly small amount of deuterium-exchanged ethane. A separate experiment showed that the exchange reaction between methane and D_2 was also negligible at this temperature.

The equilibration between H_2 and D_2 was also separately examined at temperatures between 170 K and 573 K, and was found to take place rapidly on $LaCoO_3$ with activation energy of 16.0 kJ·mol^{-1}. The rate of equilibration was about 100 times as large as that of ethylene hydrogenation at 573 K.

Catalytic behavior of Component Oxides, La_2O_3 and Co_2O_3. The catalytic activities of La_2O_3 and Co_2O_3 were also examined in order to compare with that of $LaCoO_3$. La_2O_3 showed neither hydrogenation nor hydrogenolysis activity after outgassing at temperatures below 773 K, but it became catalytically active only for the hydrogenation when heated *in vacuo* at temperature as high as 973 K. Ethylene hydrogenation on thus activated La_2O_3 exhibited a maximum in the reaction rate, 2.3×10^{14} molecule·s^{-1}·cm^{-2}, at around 548 K (P_{H_2}=98.4 Torr and $P_{C_2H_4}$=13.6 Torr), giving the activation energy of −33.1 kJ·mol^{-1} above 548 K and 16.2 kJ·mol^{-1} below this temperature. It should be noted that these reaction behavior quite resembled those for the hydrogenation on $LaCoO_3$. When Co_2O_3 was evacuated at 600 K for 1 h, the hydrogenolysis of ethylene took place at 573 K to produce ethane and methane. The catalytic activity of this oxide, however, was unstable, and this was due to the reduction of Co_2O_3 to metallic cobalt during the course of reaction, since H_2O was formed, and X-ray diffraction of the oxide employed for the reaction showed characteristic peaks associated with developed cobalt metal particles. For the initial stage of reaction, rough estimation gave a rate of ethane formation, 4×10^{11} molecules·s^{-1}·cm^{-2} at 573 K, and about 30% of reacted ethylene was consumed by the direct formation of methane *via* the adsorbed ethylene.

Structural and Chemical Changes of the Catalyst. In order to see the relationship between the structure and the activity of $LaCoO_3$, the fresh catalyst, (A), the 50% deactivated catalyst by repeated run of the reaction, (B), and the completely deactivated one (C) were examined by X-ray diffraction. Each X-ray diffraction peak of samples B and C splitted into two or three peaks which appeared at lower diffraction angles. These results suggest that the activity decreases as the lattice expands to some extent.

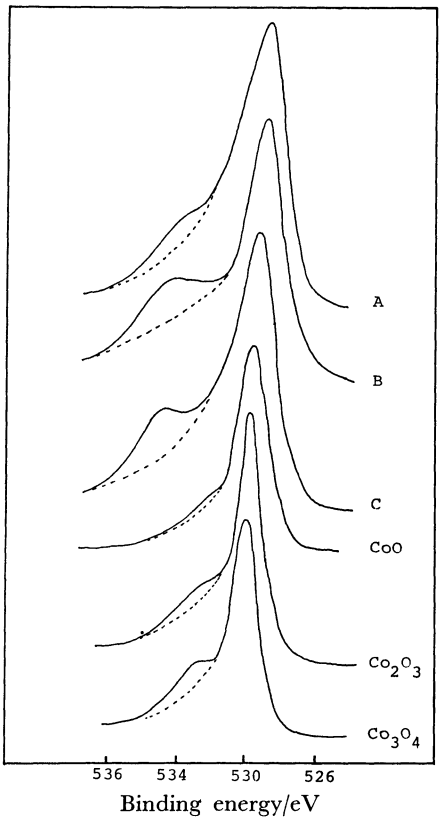

Fig. 3. X-Ray photoelectron spectra in O 1s region. Spectra A, B, and C denote the fresh $LaCoO_3$, the 50%-deactivated catalyst and the completely deactivated one, respectively.

The electronic states of samples A, B, and C were also inspected by means of XPS in comparison with those of CoO, Co_3O_4, and Co_2O_3. The O 1s spectra are illustrated in Fig. 3. The spectra of these $LaCoO_3$ samples evacuated at 300 K indicate the presence of two kinds of oxygen species; the O 1s peak of lower binding energy shifted to higher energy side with decreasing activity and the spectrum of sample became similar to those of cobalt oxides. The O 1s peak of higher binding energy diminished in intensity to the level shown by the dotted lines upon evacuation at 770 K. From the comparison with the spectra of Cu_2O, CuO, and NiO obtained by Robert *et al.*,[13] this peak was assigned to the adsorbed oxygen and the peak of lower binding energy to the lattice oxygen.

Figure 4 shows the spectral peaks from Co 2p levels. The values of spin-orbit splitting and FWHM for the fresh $LaCoO_3$ (A) are 15.3 eV and 3.2 eV, respectively, and the value of the splitting is simialr to that for Co_2O_3, 15.2 eV. However, the corresponding spectrum of catalyst C, in which the respective values are 15.9 eV and 4.7 eV, is almost the same as that of CoO with those values of 16.0 eV and 4.7 eV and is accompanied by the characteristic shake-up satellites. These differences can be used to distinguish the oxidation states of Co atoms, as reported

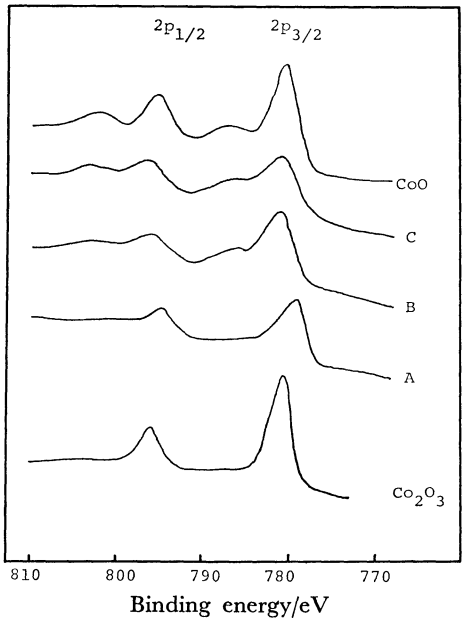

Fig. 4. X-Ray photoelectron spectra in Co 2p region. Spectra A, B, and C: see caption in Fig. 3.

by several workes,[14-16] and lead to the conclusion that the reduction from a trivalent ion, Co^{3+}, to a bivalent ion, Co^{2+}, occurred, resulting in the structural change and the degradation of catalytic activity.

No significant change of La 3d spectra was observed for all the catalysts in comparison with that for La_2O_3.

The property of $LaCoO_3$ surface was inspected from the adsorption of H_2, C_2H_4 and CO at room temperature. All the adsorbed species were removed on heating at 600 K and, from the amounts for saturation, the number of adsorption sites was estimated at 4×10^{14} cm^{-2} which corresponds to about 40% of the total surface ions.

Discussion

Mechanism of Ethylene Hydrogenolysis. The hydrogenolysis of ethylene proceeds in the following sequence;

$$\begin{array}{ccc} & C_2H_4 & \\ {\scriptstyle +H_2}\swarrow{\scriptstyle k_1} & & {\scriptstyle +2H_2}\searrow{\scriptstyle k_2} \\ & {\scriptstyle +H_2} & \\ C_2H_6 & \xrightarrow[k_3]{} & 2CH_4 \end{array}$$

Since the observed hydrocarbon orders were unity for both the hydrogenation of ethylene and the hydrogenolysis of ethane in the high temperature range and the reacting system contained a large excess of hydrogen, the rates of ethylene and ethane consumption are expressed in the form of the pseudo-first order reaction,

$$\frac{d[C_2H_4]}{dt} = -(k_1+k_2)[C_2H_4], \quad (4)$$

$$\frac{d[C_2H_6]}{dt} = +k_1[C_2H_4] - k_3[C_2H_6], \quad (5)$$

$$\frac{d[CH_4]}{dt} = +2k_2[C_2H_4] + 2k_3[C_2H_6]. \quad (6)$$

The apparent rate constants, k_1, k_2, and k_3 as parameters, were determined by applying the nonlinear least square method to the experimental data. Estimated value of k_2, 0.014 h^{-1}, was smaller than k_1, 0.15 h^{-1}, which clearly indicates that the direct conversion of C_2H_4 to CH_4 gives a minor contribution to the entire reaction. The value of k_3, 0.12 h^{-1}, was found to coincide with the rate constant evaluated from the hydrogenolysis of ethane under the same conditions. By using these parameters, the changes in the partial pressures of reactants and products with time were calculated as shown in Fig. 1. A good agreement between the observed and calculated curves confirmed that the hydrogenolysis of ethylene proceeds consecutively, as shown in the sequence,

$$C_2H_4 \xrightarrow{+H_2} C_2H_6 \xrightarrow{+H_2} 2CH_4. \quad (7)$$

The reaction of ethylene with deuterium in the high temperature region showed wide deuterium distributions in ethylene and ethane as well as the nearly established equilibrium among gaseous H_2, HD, and D_2. Thus, these results lead to the associative mechanism which involves the following reaction steps:

$$H_2 \rightleftharpoons 2H(a) \quad (8)$$

$$C_2H_4 \rightleftharpoons C_2H_4(a) \quad (9)$$

$$C_2H_4(a) + H(a) \rightleftharpoons C_2H_5(a) \quad (10)$$

$$C_2H_5(a) + H(a) \longrightarrow C_2H_6 \quad (11)$$

where (a) denotes the adsorbed state. The above-mentioned deuterium distributions also indicate that Step 11 is a rate-determining process, and the reaction rate is given by

$$R_h = k_{11}\theta_{C_2H_5}\theta_H = \frac{k_{11}K_{10}K_eK_hP_{C_2H_4}P_{H_2}}{(1+K_eP_{C_2H_4}+\sqrt{K_hP_{H_2}}+K_{10}K_eP_{C_2H_4}\sqrt{K_hP_{H_2}})^2} \quad (12)$$

where θ_i represents the fraction of surface coverage of the i species on the hydrogenation site. Under the condition of

$$1 \gg K_eP_{C_2H_4} + \sqrt{K_hP_{H_2}} + K_{10}K_eP_{C_2H_4}\sqrt{K_hP_{H_2}}, \quad (13)$$

Eq. 12 is simplified to

$$R_h = k_{11}K_{10}K_eK_hP_{C_2H_4}P_{H_2} = k_hP_{C_2H_4}P_{H_2}. \quad (14)$$

In the low temperature region, the fraction of gaseous H_2 and HD was small in contrast to the wide deuterium distributions in the ethylene and ethane, which leads to the assumption that the adsorption of hydrogen in Step 8 is a slow step. Thus, the rate equation is expressed as

$$R_1 = k_8P_{H_2}(1-\theta_{C_2H_4})^2 = \frac{k_8P_{H_2}}{(1+K_eP_{C_2H_4})^2}. \quad (15)$$

Under the condition of

$$1 \gg K_eP_{C_2H_4}, \quad (16)$$

Eq. 15 becomes

$$R_1 = k_8P_{H_2}. \quad (17)$$

Equations 14 and 17 are in agreement with the observed pressure dependences in respective temperature regions.

It is of nessesity to assess this mechanism in con-

nection with that of ethylene and ethane hydrogenolysis. The striking features of catalysis by $LaCoO_3$ were the restriction imposed on the direct path from adsorbed ethylene to methane and were also the feasibility of ethane hydrogenolysis without producing ethylene in the gas phase. With this in mind, Step 10 in the associative mechanism would appear to contradict the behavior of the hydrogenolysis, if the available sites are the same for both reactions, since the intermediate described in Step 10 would rapidly undergo the rupture of carbon-carbon bond, which turned out to give a direct pathway for methane formation. Thus, it is suggested that the active sites for hydrogenation are different from those for the hydrogenolysis. A comparison of ethylene hydrogenation on La_2O_3 and $LaCoO_3$ indicated that the kinetic behavior was quite similar each other and that the catalytic acitivity was compatible when it was evaluated as the reaction rate per La^{3+} ion exposed at surface. On the contrary, Co_2O_3 exhibited a considerable selectivity to the hydrogenolysis of the adsorbed ethylene to methane but much lower activity for the hydrogenation. Therefore, these findings enable us to conclude that a pair of La and oxygen ions is mainly responsible for the hydrogenation activity of $LaCoO_3$. In this regard, it should be noted that the conditions, (13) and (16), are established for these sites of $LaCoO_3$ oxide.

Mechanism of Hydrogenolysis of Ethane. In the hydrogenolysis of ethane over transition metals, Sinfelt *et al.* proposed the mechanism involving the dissociative adsorption of ethane to produce ethyl radical which changed to hydrogen-deficient species and further to monocarbon surface fragments.[17] In the hydrogenolysis on $LaCoO_3$, however, emphasis should be put on the results that no ethylene is formed during the reaction. The facts that the hydrogenolysis of ethane is catalyzed by Co_2O_3 but not La_2O_3, and that the H_2-D_2 equilibration takes place on these oxides and $LaCoO_3$ suggest the co-functional role of component ions in the hydrogenolysis; Co^{3+} ion is mainly responsible for the C–C bond scission, while the other La^{3+} and O^{2-} ions contribute as the sites to supply the dissociatively adsorbed hydrogen. Thus, by taking the above-mentioned pathway of ethylene hydrogenation and these findings into consideration, we propose the following reaction mechanism.

$$H_2 \rightleftharpoons 2H(a) \tag{18}$$

$$C_2H_6 + H(a) \longrightarrow CH_3(a^*) + CH_3(a^*)\cdots H(a) \tag{19}$$

$$CH_3(a^*) \rightleftharpoons CH_2(a^*) + H(a) \tag{20}$$

$$CH_3(a^*) + H(a) \longrightarrow CH_4 \tag{21}$$

where (a*) represents the adsorbed state on Co^{3+} site and (a) denotes that on La^{3+} or O^{2-} site. Since methane[D_4] is the main species in the reaction of C_2H_6 with D_2, the hydrogenolysis comprise necessarily a rapid hydrogen exchange, as expressed in Eq. 20, between surface monocarbon species, *i.e.*, adsorbed carbene and methyl radicals. The absence of deuterium-exchanged ethane strongly suggests that the Step (19) is rate-determining, and the rate equation of hydrogenolysis is given by

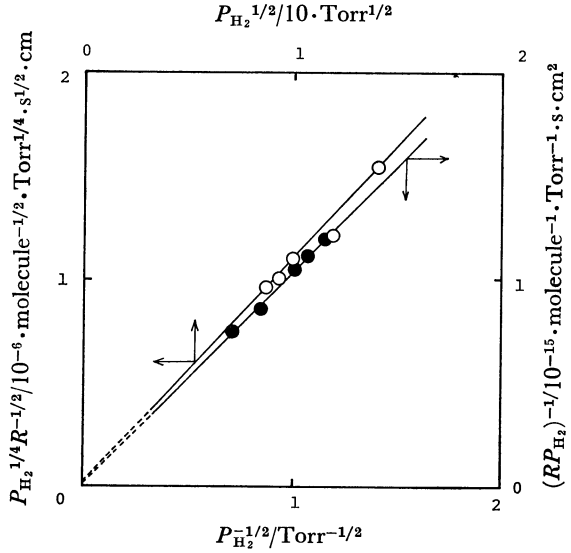

Fig. 5. Plots of $P_{H_2}^{1/4}\,R^{-1/2}$ *vs.* $P_{H_2}^{1/2}$ and $(RP_{H_2})^{-1}$ *vs.* $P_{H_2}^{-1/2}$. R and P_{H_2} represent the initial rate and the partial pressure, respectively.

$$R = k_{19}P_{C_2H_6}\theta_v^{*2}\theta_H \tag{22}$$

where θ_v^* denotes a fraction of vacant Co^{3+} sites and θ_H represents that of the other sites occupied by hydrogen atoms. These fractions are respectively described as

$$\theta_v^* = 1/(1+\sqrt{K_h^*P_{H_2}}) \text{ and } \theta_H = \sqrt{K_hP_{H_2}}/(1+\sqrt{K_hP_{H_2}}), \tag{23}$$

provided the fraction of sites covered with hydrocarbon species to be negligible. Under the condition of strong hydrogen adsorption on Co^{3+} sites, $1 \ll \sqrt{K_h^*P_{H_2}}$, the rate equation is rewritten into the form as,

$$\frac{1}{RP_{H_2}} = (K_h^*/k_{19}\sqrt{K_h}P_{C_2H_6})(\sqrt{K_h}+1/\sqrt{P_{H_2}}). \tag{24}$$

Under the condition of $1 \gg \sqrt{K_hP_{H_2}}$ as an approximation of weak adsorption on the other sites, on the other hand, the rate equation is recasted into the form

$$P_{H_2}^{1/4}/\sqrt{R} = (K_h^*/k_{19}\sqrt{K_h}P_{C_2H_6})^{1/2}(1/\sqrt{K_h^*}+\sqrt{P_{H_2}}). \tag{25}$$

Figure 5 shows good linear relationships for the plots of $(RP_{H_2})^{-1}$ *vs.* $P_{H_2}^{-1/2}$ on Eq. 24 and $P_{H_2}^{1/4}/\sqrt{R}$ *vs.* $\sqrt{P_{H_2}}$ on Eq. 25. Since the evaluated values of K_h and K_h^* at 573 K are 4×10^{-6} and 10, respectively, and P_{H_2} is 100 Torr, the relation

$$\sqrt{K_h^*P_{H_2}} \gg 1 \gg \sqrt{K_hP_{H_2}}$$

is held, which justifies the approximations used. By introducing these approximations, the rate equation (22) is finally simplified as

$$R = k_{19}\frac{\sqrt{K_h}}{K_h^*}P_{C_2H_6}P_{H_2}^{-0.5} \tag{26}$$

which accords with the observed partial pressure dependence.

It is interesting to compare the activity of $LaCoO_3$ for the hydrogenolysis of ethane with those of platinum and palladium; the specific rate for the hydrogenolysis over $LaCoO_3$ at 573 K is evaluated at 1×10^{13} molecule$\cdot s^{-1}\cdot cm^{-2}$ by using a reactant mixture of C_2H_6 (10 Torr) and H_2 (100 Torr). The values for Pt and

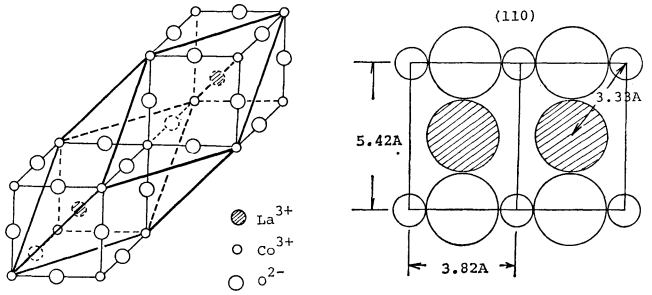

Fig. 6. Structure and geometry of $LaCoO_3$. $LaCoO_3$ have a perovskite structure, D^6_{3d}-$R_{\bar{3}m}$, but the (110) plane is drawn as cubic structure for simplicity.

Pd catalysts are respectively 2×10^{11} and 4×10^{11} molecule·s^{-1}·cm^{-2} which were obtained by correcting the Sinfelt's data[17] to the present reaction conditions. As the reaction temperature rises, the difference among these rates will be smaller because of large activation energy for Pt and Pd, *i.e.*, 227 and 244 kJ·mol^{-1}, respectively.

Structure of Active Sites. At present, knowledge on $LaCoO_3$ catalyst has not been accumulated sufficiently to mention the nature of active sites for the hydrogenolysis in detail. We give here only a speculative description to their structure and behavior. The number of adsorption sites for hydrogen or ethylene on $LaCoO_3$ corresponds to about 40% of the total surface ions. These results predict that most of the exposed surface are available for the reaction and, especially, the (110) lattice plane as illustrated in Fig. 6 is likely the most favorable for the catalysis. Among the ion pairs of Co^{3+}–O^{2-} (1.91 Å), La^{3+}–O^{2-} (2.71 Å), and La^{3+}–Co^{3+} (3.16 Å), the former two pairs seem to be suited for the dissociative adsorption of hydrogen as seen in the case of transition metal oxides. As mentioned earlier, the hydrogenation mainly proceeds on the sites consisting of La and oxygen ions. It is likely that the Co^{3+} ion in $LaCoO_3$ somewhat affects the surface states of both ions in a way to provide the hydrogenation activity in accordance with a trend that a heat treatment at high temperature changed La_2O_3 to be catalytically active. For the hydrogenolysis, the geometric arrangement of the (110) plane substantiates the co-functional role in which the Co^{3+} ion ruptures the carbon-carbon bond, and the nearby La and oxygen ions supply hydrogen atoms to the resulting monocarbon species. These synergetic effect by the three component ions in $LaCoO_3$ was found to be pronounced in the hydrogenolysis of C_3 to C_5-alkanes with longer carbon chains.[18]

The thermal desorption and IR studies of adsorbed species on $LaCoO_3$ are in progress, and the obtained information will be useful in revealing the contributions of these species to the reaction and the function of active sites.

References

1) L. A. Pedersen and W. F. Libby, *Science*, **175**, 1355 (1972).
2) R. J. H. Voorhoeve, J. P. Remeika, P. E. Freeland, and B. T. Mattias, *Science*, **177**, 353 (1972).
3) R. J. H. Voorhoeve, J. P. Remeika, L. E. Frimble, A. S. Cooper, F. J. Dialvo, and P. K. Gallagher, *J. Solid State Chem.*, **14**, 395 (1975).
4) T. Shimizu, T. Nishida, and Y. Moriwaka, *Nippon Kagaku-Kaishi*, **1974**, 1836.
5) Y. Y. Yao, *J. Catal.*, **36**, 266 (1975).
6) S. Ishiyama, Tokyo Institute of Technology M. Thesis (1975).
7) R. J. H. Voorhoeve, C. K. N. Patel, L. E. Trimble, R. J. Kerl, and P. K. Gallagher, *J. Catal.*, **45**, 297 (1972).
8) J. B. Goodenough and P. M. Raccah, *J. Appl. Phys.*, **36**, 1031 (1965).
9) L. F. Mattheiss, *Phys. Rev.*, **6**, 4718 (1972).
10) V. G. Bhide and D. S. Rajaria, *Phys. Rev. B*, **6**, 1021 (1972).
11) E. A. Kraut, T. Wolfram, and W. Hall, *Phys. Rev. B*, **6**, 1499 (1972).
12) F. Askham, I. Fankuchen, and R. Ward, *J. Am. Chem. Soc.*, **72**, 3799 (1950).
13) T. Robert, M. Bartel, and G. Offergelt, *Surface Sci.*, **33**, 123 (1972).
14) D. C. Frost, A. Ishitani, and C. A. McDowell, *Mol. Phys.*, **24**, 861 (1972).
15) D. Briggs and V. A. Gibson, *Chem. Phys. Lett.*, **25**, 493 (1974).
16) Y. Okamoto, N. Nakano, T. Imanaka, and S. Teranishi, *Bull. Chem. Soc. Jpn.*, **48**, 1163 (1975).
17) J. H. Sinfelt, *Adv. Catal.* **23**, 91 (1973).
18) K. Ichimura, Y. Inoue, and I. Yasumori, unpublished.